ISSN 1063-7850, Technical Physics Letters, 2007, Vol. 33, No. 11, pp. 919–922. © Pleiades Publishing, Ltd., 2007.
Original Russian Text © N.G. Chechenin, P.N. Chernykh, V.S. Kulikauskas, Y. Pei, D. Vainshtein, J.Th.M. De Hosson, 2007, published in Pis'ma v Zhurnal Tekhnicheskoĭ Fiziki, 2007, Vol. 33, No. 21, pp. 47–55.

Determining the Mass Density of a Hydrocarbon Matrix in Thin-Film Nanocomposites by Ion-Beam Techniques

N. G. Chechenin*, P. N. Chernykh, V. S. Kulikauskas, Y. Pei, D. Vainshtein, and J. Th. M. De Hosson

Skobel'tsyn Institute of Nuclear Physics, Moscow State University, Moscow, 119899 Russia
Materials Science Center, University of Groningen, 9747 AG Groningen, The Netherlands
**e-mail: chechenin@sinp.msu.ru*

Received January 12, 2007; in final form, April 18, 2007

Abstract—An approach based on ion-beam analysis, including Rutherford backscattering, nuclear backscattering, and elastic recoil detection, for determining the partial mass density of a hydrocarbon matrix in nanocomposites is proposed and applied to the nc-TiC/a-C:H thin-film coating material.

PACS numbers: 61.18.Bn, 81.07.-b

DOI: 10.1134/S1063785007110089

Hydrogen-containing amorphous carbon nanocomposites containing dispersed foreign nanocrystalline grains have been extensively studied in recent years. These coating materials are characterized by large variability of their functional properties, including electrical characteristics, corrosion resistance, mechanical properties (hardness, strength, elastic moduli, low friction coefficient), etc. The combination of properties of the a-C:H base (matrix) and the whole coating are determined to a considerable extent by the ratio of diamondlike sp^3 bonds and graphitelike sp^2 bonds. There is evidence that hydrogen also plays a significant role in this system, by stimulating the formation of diamondlike sp^3 bonds [1, 2]. On the contrary, the loss of hydrogen (e.g., as a result of annealing) leads to the transformation of sp^3 bonds into sp^2 bonds [3, 4]. The bonds in these diamondlike carbon (DLC) composites are most frequently studied using Raman and IR spectroscopy, X-ray photoelectron spectroscopy [5], or more sophisticated techniques such as electron energy loss spectroscopy [6]. Despite the variety of available methods, quantitative determination of the fractions of sp^3 and sp^2 bonds is not a simple problem having an unambiguous solution. Another difficult task is determining the hydrogen in the coating material. The unique possibility of straightforward nondestructive hydrogen determination is offered by methods of ion-beam analysis (IBA), in particular, by elastic recoil detection (ERD) [7].

In the present investigation, various IBA techniques have been used for a complex analysis of the elemental composition of a DLC coating: Rutherford backscattering (RBS) and nuclear backscattering (NBS) were used to study the distribution of titanium and carbon, while ERD was used to determine the concentration of hydrogen. In addition to the complex use of IBA methods for the investigation of composition, we take the next step in DLC characterization by proposing a method for determining the partial mass density of the hydrocarbon matrix in the nanocomposite, which cannot be achieved by any other means. This method provides an alternative approach to the analysis of the sp^3/sp^2 bond ratio in the a-C:H matrix and the elucidation of its influence on the functional properties of DLC coatings. The proposed method will be demonstrated by application to a thin-film nanocomposite comprising a hydrogen-containing amorphous carbon (a-C:H) matrix with dispersed titanium carbide (TiC) nanoparticles: nc-TiC/a-C:H.

The coating was deposited in a Hauzer NTC-1000 system using magnetron sputtering in a closed unbalanced magnetic field (CFUBMS) in an Ar/acetylene atmosphere. The film composition was studied by RBS, NBS, and ERD methods using 2.3-MeV He^+ and 1.5-MeV H^+ ion beams. Figure 1 shows the typical RBS spectrum obtained with 2.3-MeV He^+ ions for an a-C:H(TiC) coating deposited onto a Cr/Si substrate. The channel number characterizes the energy of backscattered ions. Due to a difference in the kinematic factors K for ions scattered from titanium and carbon, the signals from these components in Fig. 1 are shifted in energy. The presence of a shift relative to the position determined by the kinematic factor for elements such as Cr and Si (Fig. 1) is related to the depth of these layers in the sample. The height H_i of the partial spectrum for a given element i is determined by the cross section $d\sigma_i/d\Omega$ and the concentration (or atomic density) N_i of this element and can be approximately described by the equation

$$H_i = Q\Omega(d\sigma_i(\theta)/d\Omega)N_i\delta E/\{[dE/dx)_i]\cos\theta_{in}\}, \quad (1)$$

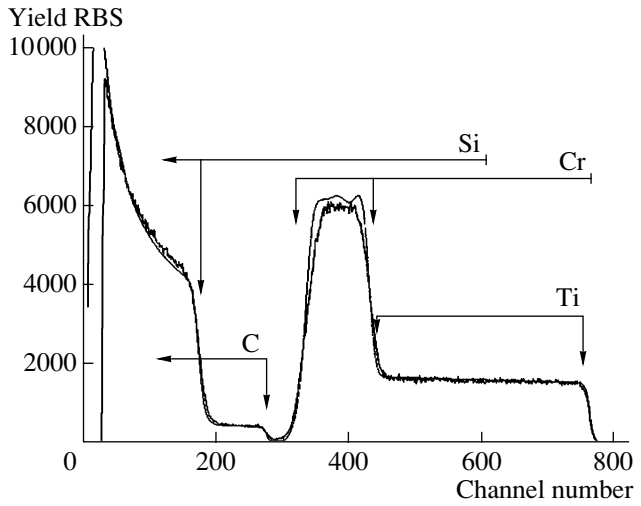

Fig. 1. The typical experimental 2.3-MeV He^+ RBS spectrum (noisy curve) and a simulated (RUMP [9]) spectrum (smooth curve) of a $Ti_{31}C_{54}H_{33}$/Cr/Si sample. Arrows pointing downward indicate the localization of elemental contributions; the beginning of arrows corresponds to the energy of scattered ions for scattering atoms situated on the surface.

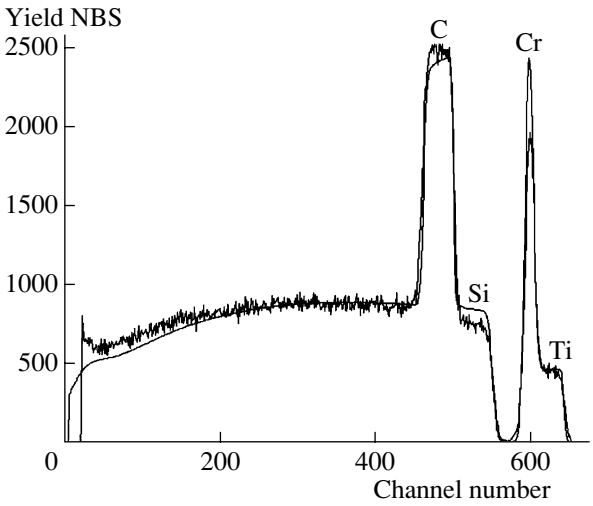

Fig. 2. The typical experimental 1.5-MeV H^+ NBS spectrum (noisy curve) and a simulated (RUMP [9]) spectrum (smooth curve) of a $Ti_{12}C_{57}H_{31}$/Cr/Si sample.

where Q *i*s the total number of ions in the probing beam striking the target during accumulation of the spectrum; Ω is the solid angle of the detector; θ_{in} is the incidence angle (measured between the normal to the sample surface and the primary ion beam direction); δE is the energy width of a channel; $[(dE/dx)_i]$ is the ion energy losses for the forward and reverse motion,

$$[(dE/dx)_i] = \Sigma_j N_j[(K_i/\cos\theta_{in})\varepsilon_j(\langle E_{in}\rangle) + (1/\cos\theta_{out})\varepsilon_j(\langle E_{out}\rangle)]; \quad (2)$$

ε_j is the stopping cross section in the jth medium; $\langle E_{in}\rangle$ and $\langle E_{out}\rangle$ are the average energies of the incoming and outgoing particle on the forward and reverse trajectories, respectively; and θ_{out} is the escape angle (measured between the normal to the sample surface and the direction to the detector). Equations (1) and (2) serve as a basis for the elemental analysis of materials in terms of the relative concentrations N_i/N_j or $c_i = N_i/N_0$, where $N_0 = \Sigma_i N_i$ is the total atomic density of the analyzed substance. The smooth curve in Fig. 1 shows the simulated RBS spectrum obtained using the RUMP program [9], where the calculation is performed for the sample film separated into layers sufficiently thin to satisfy the thin layer approximation used in the formulation of Eqs. (1) and (2).

Equations (1) and (2) are also applicable to the NBS analysis. The main difference between RBS and NBS is related to the corresponding cross sections. In NBS, the cross section is proportional to Z^2 and, hence, is small for light elements such as carbon. For protons with an energy above 1 MeV, the elastic cross section can be much greater than the RBS cross section, which is related to a contribution due to the nuclear cross section of the elastic process. As can be seen from Fig. 2, the contribution due to the scattering from carbon (channel nos. 450–500) exceeds those of both silicon (the level of the pedestal of the carbon peak) and titanium (frontal region).

Both RBS and NBS methods are insensitive to hydrogen since the cross section for elastic scattering on a proton is very small. On the contrary, the method employing recoil nuclei can be used only for the investigation of elements having lower masses as compared to the probing ions (He^+), that is, for hydrogen. Figure 3 shows the typical ERD spectrum obtained using 2.3-MeV He^+ ions (smooth curves show the model spectra of $C_xH_yTi_z$ for the hydrogen concentrations $y = 0.26$, 0.28, and 0.30. As can be seen, the optimum approximation of the experimental spectrum is provided by the model for $y = 0.28$, while the other two approximations are unsatisfactory.

The energy width of the interval ΔE_i in the RBS spectrum, which reflects the scattering on atoms of the ith element, also depends on the layer thickness t. In the approximation of a weak energy dependence of losses and small thicknesses, Eq. (2) yields

$$\Delta E_i = (N_0 t)\Sigma_j(N_j/N_0)[(K_i/\cos\theta_{in})\varepsilon_j(\langle E_{in}\rangle) + (1/\cos\theta_{out})\varepsilon_j(\langle E_{out}\rangle)]. \quad (3)$$

This relation allows the layer thickness to be determined in units of the surface atomic density N_0t. For example, in the RBS spectrum of a $C_xH_yTi_z$ coating (Fig. 1), one can readily determine the width of the interval ΔE_{Ti} related to the scattering on Ti atoms and the corresponding surface atomic density .

If the coating thickness is known (e.g., as t_{SEM} from scanning electron microscopy (SEM) data on the sam-

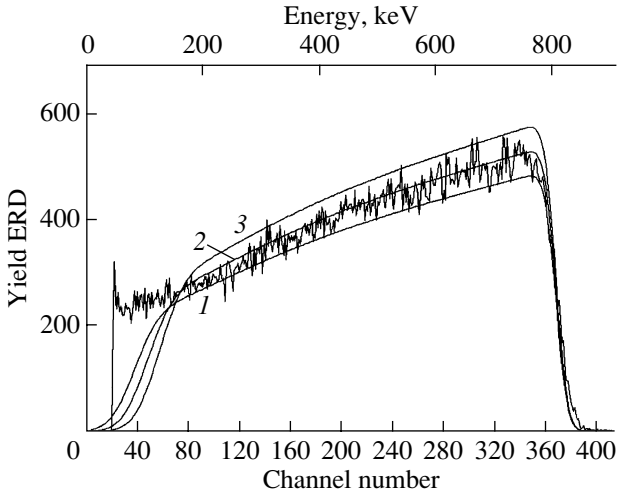

Fig. 3. The typical experimental 2.3-MeV He^+ ERD spectrum (noisy curve) and simulated spectra (smooth curves) for (*1*) $Ti_{10}C_{64}H_{26}$, (*2*) $Ti_{10}C_{62}H_{28}$, and (*3*) $Ti_{10}C_{60}H_{30}$.

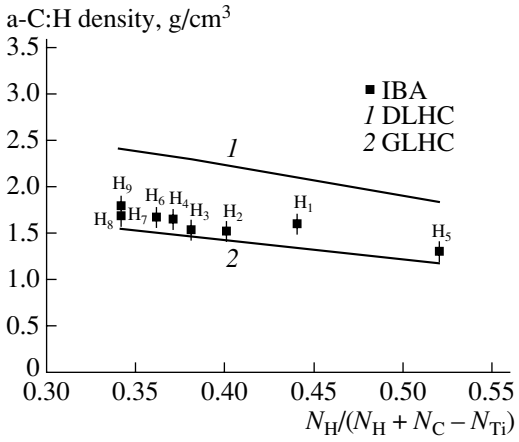

Fig. 4. Experimental (squares) and theoretical (curves) dependences of the mass density ρ_{D-H} of the matrix on the percentage content of hydrogen for hydrogen substituting carbon in (*1*) DLHC and (*2*) GLHC bonds.

ple cross section) and the surface atomic density is measured by RBS as $(N_0t)^{RBS}$, the absolute volume atomic density can be determined as

$$N_0 = (N_0t)^{RBS}/t_{SEM}. \quad (4)$$

Investigations showed that, owing to a high cohesion ($\Delta H = -231.7$ kJ/mol [10]), Ti and C atoms form quasi-molecules with dimensions from 2 to 5 nm [8]. Then, the system $C_xH_yTi_z$ with $x > z$ and $x + y + z = 1$ can be represented as a system of quasi-molecular clusters $(TiC)_z$ and matrix molecules $C_{x-z}H_y$. In this case, the general formula of the system can be rewritten as $(CH_{y/(x-z)})_{x-z}(TiC)_z$. Evidently, this coating contains zN_0TiC quasi-molecules TiC with the molar weight $M_{TiC} = 59.9$ and $(x - z)N_0$ quasi-molecules $CH_{y/(x-z)}$ with the molar weight $M_{CH} = 12 + 1(1 - x - z)/(x - z)$. The partial atomic densities are $N_C = xN_0$, $N_H = yN_0$, and $N_{Ti} = zN_0$. The atomic and mass density in TiC clusters is the same as in crystalline TiC ($\rho_{TiC} = 4.92 \approx 4.9$ g/cm^3), while the density of the C–H amorphous matrix is a priori unknown. However, this value can be estimated using RBS and electron-microscopic data as

$$\rho_{CH} = m_{CH}/V_{CH} = (x-z)N_0M_{CH}m_0/(1 - zN_0M_{TiC}m_0/\rho_{TiC}), \quad (5)$$

where $m_{CH} = N_{CH}(\text{mol/cm}^3)M_{CH}(\text{u/mol})m_0(\text{g/u}) = (x - z)N_0M_{CH}m_0(\text{g})$ is the specific mass of the CH matrix in the coating, $V_{CH} = 1 - V_{TiC} = 1 - zN_0M_{TiC}m_0/\rho_{TiC}$ is the specific volume (cm^3) occupied by the CH matrix (after subtraction of the specific volume of TiC), and $m_0 \approx 1.66 \times 10^{-24}$ g/u is the mass of 1 u.

Figure 4 shows the results of analysis of the density of the CH matrix performed as described above, plotted versus percentage content of hydrogen. As can be seen, the matrix density falls within 1.5–1.9 g/cm^3 and decreases with increasing percentage content of hydrogen in the coating. The values of density are significantly smaller compared to the density of a diamond coating (3.5 g/cm^3) even with allowance for the fact that hydrogen partly substitutes for carbon. This substitution of hydrogen for carbon in sp^3 bound diamondlike hydrocarbon (DLHC) can be taken into account using the following simplified formula:

$$\rho_{D-H} = \rho_D\left(\frac{1 + \frac{M_H}{M}\frac{N_H}{(N_C - N_{Ti})}}{1 + \frac{N_H}{(N_C - N_{Ti})}}\right), \quad (6)$$

where ρ_D and ρ_{D-H} are the densities of diamond and DLHC, respectively. The dependence of ρ_{D-H} on the hydrogen content is depicted in Fig. 4 (curve *1*).

Alternatively, it is possible to estimate the density of the CH matrix assuming that hydrogen substitutes for carbon in sp^2 bound graphitelike hydrocarbon (GLHC). The density of graphite exhibits a significant spread (from 1.6 to 2.25 g/cm^3), which is related to the strong dependence of graphite structure on the technology of synthesis [11]. Figure 4 (curve *2*) shows the GLHC density ρ_{G-H} as a function of the substitution in (6), calculated assuming the most dense graphite packing ($\rho_G = 2.25$ g/cm^3).

Comparing the DLHC and GLHC dependences to the experimental density, it is possible to evaluate the ratio of diamondlike (fsp^3) and graphitelike (fsp^2) frac-

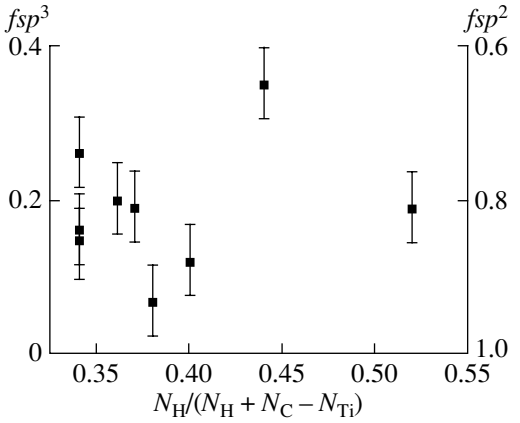

Fig. 5. A plot of the diamondlike (fsp^3) and graphitelike (fsp^2) fractions versus hydrogen content in nc-TiC/a-C:H.

tions. Assuming that fsp^3 is proportional to ρ_{D-H} and fsp^2 is proportional to ρ_{G-H}, we obtain

$$fsp^3 = (\rho_{exp} - \rho_{G-H})/(\rho_{D-H} - \rho_{G-H}) \quad (7)$$

and

$$fsp^2 = 1 - fsp^3.$$

A plot of this dependence in Fig. 5 shows that the GLHC bond is obviously dominating. However, the DLHC bond exhibits the tendency to grow with decreasing hydrogen content.

In conclusion, we have demonstrated that, using ion-beam diagnostics supplemented by some other methods such as SEM, it is possible to determine an important parameter of a hydrocarbon nanocomposite coating such as the ratio of diamondlike and graphitelike bond fractions.

Acknowledgments. This study was supported by the Presidential Program for Support of Leading Scientific Schools in Russia (project no. NSh-1619.2003.2) and performed within the framework of the Agreement on Research Collaboration between the Skobel'tsyn Institute of Nuclear Physics (Moscow State University, Russia) and the Materials Science Center (University of Groningen, The Netherlands).

REFERENCES

1. B. Dischler, A. Bubenzer, and P. Koidl, Solid State Commun. **48**, 105 (1983).
2. T. Mikami, H. Nakazawa, M. Kudo, and M. Mashita, Thin Solid Films **488**, 87 (2005).
3. N. M. J. Conway, A. C. Ferrari, A. J. Flewitt, et al., Diamond Relat. Mater. **9**, 765 (2000).
4. H. Li, T. Xu, C. Wang, et al., Thin Solid Films **515**, 2153 (2006).
5. J. Robertson, Mater. Sci. Eng., R **37**, 129 (2002).
6. D. Galvan, Y. T. Pei, J. Th. M. De Hosson, and A. Cavaleiro, Surf. Coat. Technol. **200**, 739 (2005).
7. V. Rigato, G. Maggioni, D. Boscarino, et al., Surf. Coat. Technol. **116–119**, 580 (1999).
8. Y. T. Pei, D. Galvan, and J. Th. M. De Hosson, Acta Mater. **53**, 4505 (2005).
9. L. R. Dolittle, Nucl. Instrum. Methods Phys. Res. B **9**, 344 (1985).
10. *Chemical Encyclopedia* (Sov. Éntsiklopediya, Moscow, 1990), Vol. 2 [in Russian].
11. *Chemical Encyclopedia* (Sov. Éntsiklopediya, Moscow, 1988), Vol. 1 [in Russian].

Translated by P. Pozdeev